

Foldseek: fast and accurate protein structure search

Michel van Kempen,^{1,*} Stephanie S. Kim,^{2,*} Charlotte Tumescheit,²
Milot Mirdita,¹ Johannes Söding,^{1,3,†} and Martin Steinegger^{2,4,†}

Highly accurate structure prediction methods are generating an avalanche of publicly available protein structures. Searching through these structures is becoming the main bottleneck in their analysis. Foldseek enables fast and sensitive comparisons of large structure sets. It reaches sensitivities similar to state-of-the-art structural aligners while being four orders of magnitude faster. Foldseek is free open-source software available at foldseek.com and as a webserver at search.foldseek.com.

Contact: soeding@mpinat.mpg.de, martin.steinegger@snu.ac.kr

1 The recent breakthrough in *in-silico* protein structure pre-
2 diction at near-experimental quality by AlphaFold2 [1] and
3 then RoseTTAFold [2] is revolutionizing structural biology
4 and bioinformatics. The European Bioinformatics Institute
5 (EBI) in collaboration with AlphaFold2/DeepMind has al-
6 ready made 1106829 protein structures publicly available
7 and plans to extend this library to hundreds of millions of
8 structures this year [3]. With these novel computational ap-
9 proaches, it will not be long before billions of high quality pro-
10 tein structures become available [4]. The scale of this treasure
11 trove poses challenges to state-of-the-art analysis methods.

12 Currently, the most widely used approach to protein an-
13 notation and analysis is based on sequence similarity search
14 [5–8]. The goal is to find homologous sequences from which
15 properties of the query sequence can be inferred, such as
16 molecular and cellular functions and structure. Despite the
17 success of sequence-based homology inference, many proteins
18 cannot be annotated because detecting distant evolutionary
19 relationships from sequences alone remains challenging [9].

20 Detecting similarity between protein structures by 3D su-
21 perposition offers higher sensitivity for identifying homolo-
22 gous proteins [10]. The imminent availability of high-quality
23 structure models for any protein of interest could allow us
24 to use structure comparison to improve homology-based in-
25 ference and structural, functional and evolutionary analyses.
26 However, despite decades of effort to improve speed and sen-
27 sitivity of structural aligners, current tools are much too slow
28 to cope with the expected scale of structure databases.

29 For example, searching with a single query structure
30 through a database with 100 million protein structures would
31 take the popular TMalign [11] tool around a month on one
32 CPU core, and an all-versus-all comparison would take around
33 10 millennia on a 1000 core cluster. In comparison, sequence
34 searching is five orders of magnitude faster: An all-versus-
35 all comparison of 100 M sequences would take MMseqs2 [6] at
36 high search sensitivity only around a week on the same cluster.

37 Structural alignment tools are slower for two reasons. First,
38 whereas sequence search tools employ fast and sensitive pre-
39 filter algorithms to gain several orders of magnitude in speed,
40 no comparable prefilters exist for structure searches. Sec-

41 ond, structural similarity scores are non-local: changing the
42 alignment in one part affects the similarity in all other parts.
43 For example in TMalign, two highly interdependent optimiza-
44 tions are performed: The pairing up of residues that are to be
45 aligned with each other, and the superposition of the 3D struc-
46 tures by minimizing some distance measure between aligned
47 residues. Most structural aligners, such as the popular TMA-
48 lign, DALI, and CE [11–13], solve the alignment optimization
49 problem by iterative or stochastic optimization.

50 To increase speed, a crucial idea is to describe the amino
51 acid backbone of proteins as sequences over a structural alpha-
52 bet and compare structures using sequence alignments [14]. In
53 this way, structural alphabets reduce structure comparisons to
54 much faster sequence alignments. Many ways to discretize the
55 local amino acid backbone have been proposed [15]. Most,
56 such as CLE, 3D-BLAST, and Protein Blocks, discretize the
57 conformations of short stretches of usually 3 to 5 C_{α} atoms
58 [16–18]. 3D-BLAST and CLE trained a substitution matrix
59 for their structural alphabet and rely on an aligner like BLAST
60 [5] to perform the sequence searches.

61 For Foldseek, we developed a novel type of structural alpha-
62 bet that does not describe the backbone but rather tertiary
63 interactions. The 20 states of the 3D-interactions (3Di) al-
64 phabet describe for each residue i the geometric conformation
65 with its spatially closest residue j . Compared to the various
66 backbone structural alphabets, 3Di has three key advantages:
67 First, the dependency of consecutive 3Di letters on each other
68 is much weaker than for backbone structural alphabets, where
69 for instance a helix state is followed by another helix state with
70 high probability. The dependency decreases information den-
71 sity and results in high-scoring false alignments. Second, the
72 frequencies of the 3Di states are more evenly distributed than
73 for backbone states, for which 60% describe generic secondary
74 structure states. This further increases information density
75 in 3Di sequences (**Supplementary Table 1**) and decreases
76 false positives. Third, in backbone structural alphabets, less
77 information is contained in the highly conserved protein cores
78 (consisting mostly of regular secondary structure elements)
79 and more in the predominantly non-conserved coil/loop re-
80 gions. In contrast, 3Di sequences have the highest information
81 density in conserved cores and the lowest in loop regions.

82 Foldseek (**Fig. 1a**) (1) discretizes the query structures into
83 sequences over the 3Di alphabet and then searches through
84 the 3Di sequences of the target structures using the double-
85 diagonal k -mer-based prefilter and gapless alignment prefilter
86 modules from MMseqs2, our highly optimized and parallelized
87 open-source sequence search software [6]. (2) High scoring hits

* These two authors contributed equally

† Authors to whom correspondence should be addressed

¹ Quant. & Comput. Biology, Max Planck Institute for Multidisciplinary Sciences, Göttingen, Germany. ² School of Biological Sciences, Seoul National University, Seoul, South Korea. ³ Campus-Institute Data Science (CIDAS), Goldschmidtstrasse 1, 37077 Göttingen, Germany. ⁴ Artificial Intelligence Institute, Seoul National University, Seoul, South Korea

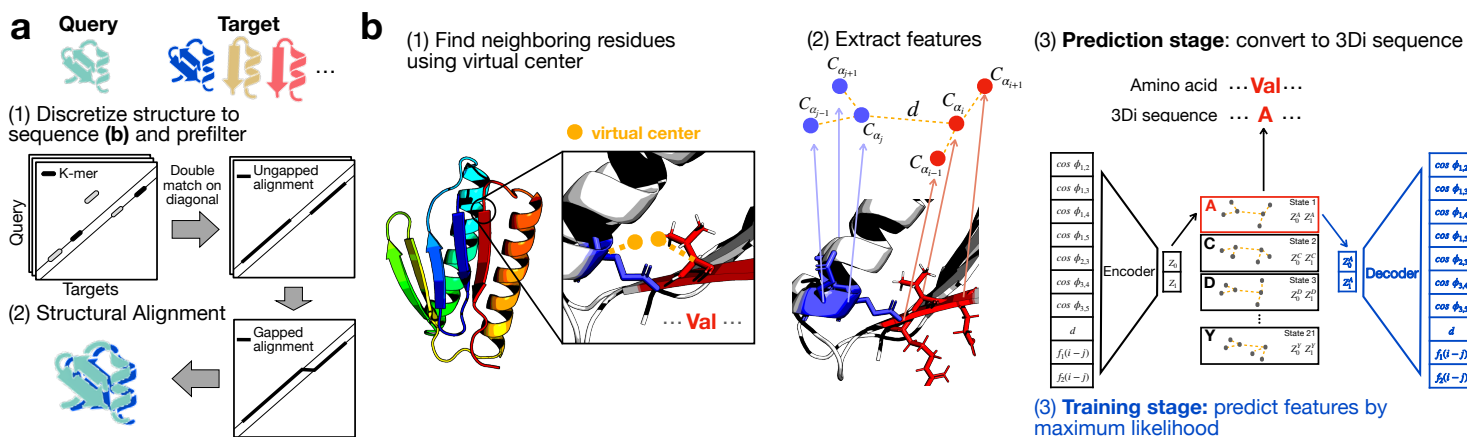


FIG. 1. Foldseek workflow. (a) Foldseek searches a set of query structures through a set of target structures. (1) Query and target structures are discretized into 3Di sequences (see b). To detect candidate structures, we apply the fast and sensitive k -mer and ungapped alignment prefilter from MMseqs2 on the 3Di sequences. (2) Followed by a local alignment using a vectorized Smith-Waterman algorithm combining both 3Di and amino acid substitution scores. Alternatively, a global alignment is computed with an accelerated TAlign version. (b) Learning the 3Di alphabet: (1) 3Di states describe tertiary interaction between a residue i and its nearest neighbor j . Nearest neighbors have the closest virtual center distance (yellow). Virtual center (Supplementary Fig. 1) positions were optimized for maximum search sensitivity. (2) To describe the interaction geometry of residues i and j , we extract seven angles, the euclidean C_{α} distance, and two sequence distance features from the six C_{α} coordinates of the two backbone fragments (blue, red). (3) These 10 features are used to define 20 3Di states by training a vector-quantized variational autoencoder [19] modified to learn states that are maximally evolutionarily conserved. For structure searches, the encoder predicts the best-matching 3Di state for each residue.

88 are aligned locally (default) or aligned globally with TAlign.
 89 align. The novel local alignment stage combines structural and
 90 amino acid substitution scores for improved sensitivity with-
 91 out sacrificing speed. The construction of the 3Di alphabet is
 92 summarized in Fig. 1b and Supplementary Figs 1–3.

93 To minimize high-scoring false positives and provide reliable
 94 E-values, for each match the score of the reversed query
 95 sequence is subtracted from the original score. Furthermore,
 96 a compositional bias correction is applied that lowers the sub-
 97 stitution scores of 3Di states enriched within a local 40 residue
 98 sequence window (see “Pairwise local structural alignments”).
 99 E-values are calculated based on an extreme-value score distri-
 100 bution whose parameters are predicted by a neural network
 101 from 3Di sequence composition and length (see “E-Values”).

102 We measured the sensitivity and speed of Foldseek and six
 103 structure alignment tools with single-domain structures (Fig.
 104 2a-b) on the SCOPe40 dataset [20]. This dataset contains
 105 11 211 protein domains clustered at 40% sequence identity.
 106 We performed an all-versus-all search and compared the per-
 107 formance for finding members of the same SCOPe family, su-
 108 perfamily, and fold (true positive matches, TPs) by measuring
 109 the fraction of TPs out of all possible correct matches for the
 110 query until the fifth false positive (FP). FPs are matches to a
 111 different fold (see “SCOPe Benchmark”). The sensitivity was
 112 measured by the area under the curve (AUC) of the cumula-
 113 tive ROC curve up to the fifth FP.

114 Foldseek reaches sensitivities at family and superfamily
 115 level below Dali, higher than the structural aligner CE, and
 116 performs similarly to TAlign and TAlign-fast. Foldseek
 117 is much more sensitive than structural alphabet-based search
 118 tools 3D-BLAST and CLE-SW (Fig. 2a-b). Even on the fold
 119 level, where most TPs are between non-homologous superfam-
 120 ilies, it is more sensitive than CE and similar to TAlign. Yet

121 on this small, single-domain benchmark it is more than 3,000
 122 times faster than TAlign, DALI, and CE (Fig. 2b). On the
 123 much larger AlphaFoldDB, where Foldseek approaches its full
 124 speed, it is around 184,600 and 23,000 faster than DALI and
 125 TAlign, respectively (Fig. 2d). Its E-values are accurate,
 126 which is critical for homology searching (Fig. 2c)

127 To assess the reliability and speed of Foldseek with full-
 128 length protein chains, we performed an all-versus-all Foldseek
 129 search on the AlphaFoldDB. For each query structure we com-
 130 puted the TAlign score of Foldseek’s second best match (the
 131 best match is the self-match). We ignored matches for which
 132 the average of the predicted Local Distance Difference Test
 133 (pLDDT [1]) from query and target is below 80 or which are
 134 fragmented. All but 1,675 out of 133,813 second-best matches
 135 with high alignment confidence (Foldseek score per aligned
 136 column ≥ 1.0) had a good TM-score (≥ 0.5), indicating that
 137 the fold was correctly recognized (Supplementary Fig. 4).
 138 Manual inspection of outliers with high Foldseek score per
 139 column and low TMscores (< 0.5) revealed Foldseek matches
 140 with multiple smaller, correctly aligned regions (Supplemen-
 141 tary Table 2). Even though their average pLDDT is above
 142 80, the relative orientation of correctly folded segments is of-
 143 ten not correctly predicted by AlphaFold2. TM-align does not
 144 identify these as homologs, as it searches for global structural
 145 superpositions, thus overlooking significant local similarities.

146 We investigated the sensitivity for detecting very remote
 147 homologs by counting the number of cross-kingdom hits within
 148 AlphaFoldDB. Foldseek and MMseqs2 found cross-kingdom
 149 hits for 34.5% and 27.4% of the 364 357 queries, respectively.
 150 Overall, Foldseek finds 3.4 times as many cross-kingdom hits
 151 as MMseqs2 (see Supplementary Fig. 5).

152 To facilitate access to Foldseek, we developed a user-
 153 friendly webserver optimized to quickly return results for sin-

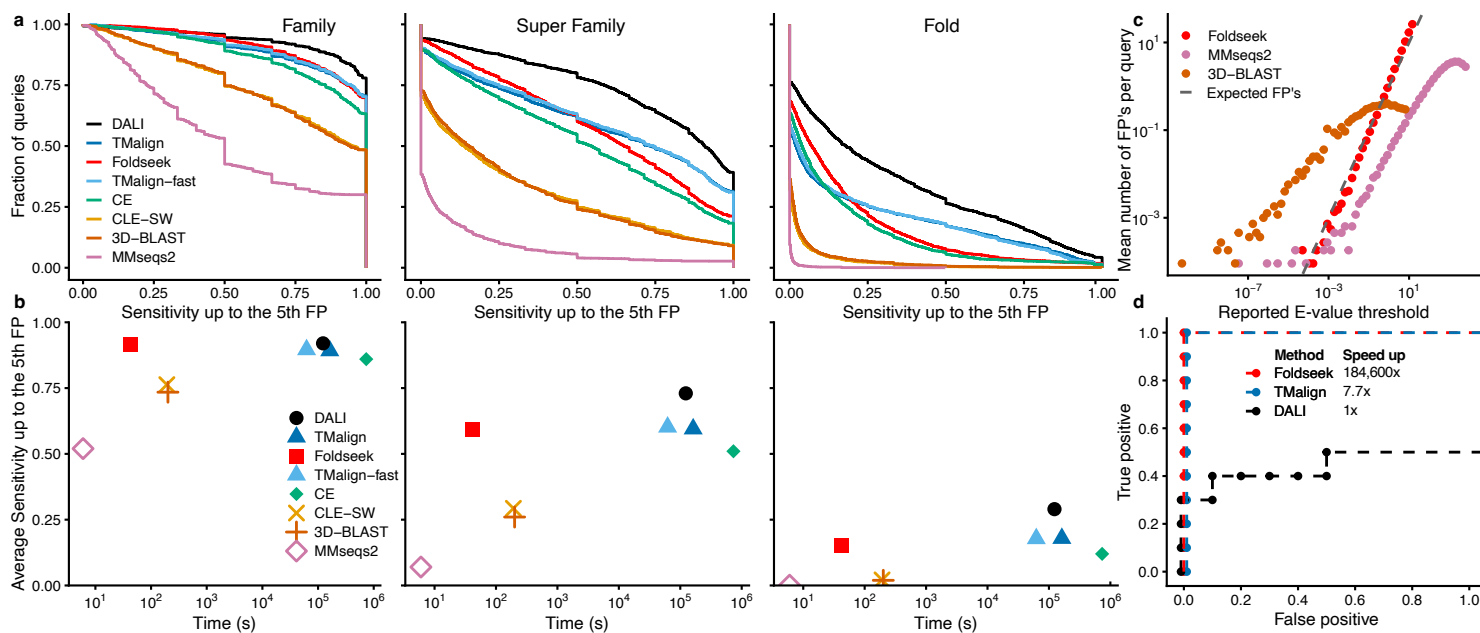


FIG. 2. Foldseek reaches similar sensitivities as structural aligners at thousands of times their speed (a) Cumulative distributions of sensitivity for homology detection. Sensitivity is the area under the ROC curve up to the fifth false positive, for all-versus-all searches with the 11 211 single-domain structures of the SCOPe40 database). True positives are matches within the same family, superfamily or fold (see main text). (b) Sensitivity versus total runtime on an AMD EPYC 7702P 64-core CPU for the all-versus-all searches. (c) Accuracy of reported E-values: Mean number of FP hits versus reported E-value threshold. (d) Top10 hits of search with RdRp (6M71_A) through the AlphaFold/Proteome with Foldseek, TMalign and DALI.

154 gle queries. It performs searches through three structure
155 databases, AlphaFoldDB/Proteome, AlphaFoldDB/Swiss-
156 Prot, and the PDB100, using one of three alignment meth-
157 ods: standard Foldseek (default), Foldseek without amino acid
158 scoring, and TMalign. The server takes PDB files as input
159 and returns a list of matched structures, query-target sequence
160 alignments, similarity scores, and E-values or TMscores.

161 We compared the Foldseek webserver with TMalign and
162 DALI by searching with the SARS-CoV-2 RNA-dependent
163 RNA polymerase (RdRp, PDB: 6M71_A [21]; 942 residues)
164 through the AlphaFoldDB (Proteome + Swiss-Prot) contain-
165 ing 804872 protein structures. The searches took TMalign
166 33h and DALI 10 days to complete on a single core. Foldseek
167 took 5 seconds, which is about 23 000, 180 600 times faster
168 than TMalign and DALI respectively. We compared the top
169 10 hits of the AlphaFoldDB/Proteome database (**Fig. 2d**).
170 Foldseek as well as TMalign contain only reverse transcrip-
171 tase (RT) domains, which are structurally similar to RdRps.
172 DALI finds three RdRp and two RT hits, and five FPs hits to
173 kinases (**Supplementary Table 3**). Foldseek finds significant
174 hits with E-values between 10^{-7} to 10^{-6} , while TMalign re-
175 ports low TM-scores between 0.419 and 0.42. This illustrates
176 a key difference between structural aligners, which depend on
177 finding a global 3D superposition, and Foldseek's local align-
178 ment. Foldseek is independent of the relative orientation of
179 domains and therefore excels at detecting homologous multi-
180 domain structures.

181 The availability of high-quality protein structures for nearly
182 every structured protein is going to be transformative for
183 structural biology and bioinformatics. What could until re-
184 cently only be done by analyzing sequences can now be done

185 with structures. The main limitation in our view, the four
186 orders of magnitude slower speed of structure comparisons, is
187 removed by Foldseek.

REFERENCES

- 189 [1] Jumper, J. *et al. Nature* **596**, 583–589 (2021).
- 190 [2] Baek, M. *et al. Science* **373**, 871–876 (2021).
- 191 [3] Varadi, M. *et al. Nucleic Acids Res* **50**, D439–D444 (2022).
- 192 [4] Burley, S. K. *et al. Nucleic Acids Res* **49**, D437–D451 (2021).
- 193 [5] Altschul, S. F. *et al. J Mol Biol* **215**, 403–410 (1990).
- 194 [6] Steinegger, M. & Söding, J. *Nat Biotechnol* **35**, 1026–1028
195 (2017).
- 196 [7] Steinegger, M. *et al. BMC Bioinform* **20**, 473 (2019).
- 197 [8] Buchfink, B. *et al. Nat Methods* **18**, 366–368 (2021).
- 198 [9] Rost, B. *Protein Eng Des Sel* **12**, 85–94 (1999).
- 199 [10] Illergård, K. *et al. Proteins* **77**, 499–508 (2009).
- 200 [11] Zhang, Y. & Skolnick, J. *Nucleic Acids Res* **33**, 2302–2309
201 (2005).
- 202 [12] Holm, L. *Methods Mol Biol* **2112**, 29–42 (2020).
- 203 [13] Shindyalov, I. N. & Bourne, P. E. *Protein Eng Des Sel* **11**,
204 739–747 (1998).
- 205 [14] Guyon, F. *et al. Nucleic Acids Res* **32**, W545–W548 (2004).
- 206 [15] Ma, J. & Wang, S. *Adv Protein Chem Struct Biol* **94**, 121–175
207 (2014).
- 208 [16] Wang, S. & Zheng, W.-M. *J Bioinform Comput Biol* **6**, 347–
209 366 (2008).
- 210 [17] Yang, J.-M. & Tung, C.-H. *Nucleic Acids Res* **34**, 3646–3659
211 (2006).
- 212 [18] de Brevern, A. G. *et al. Proteins* **41**, 271–287 (2000).
- 213 [19] Van den Oord, A. *et al. Adv Neur Inf Proc Syst (NIPS)* **30**
214 (2017).
- 215 [20] Chandonia, J.-M. *et al. Nucleic Acids Res* **47**, D475–D481
216 (2019).
- 217 [21] Gao, Y. *et al. Science* **368**, 779–782 (2020).

218

Acknowledgements

219 We thank Nicola Bordin, Ian Sillitoe and Christine Orengo
220 for reporting issues and providing valuable feedback, and
221 Yang Zhang and Marcin Wojdyr for making TMalign and the
222 Gemmi library freely accessible, and Do-Yoon Kim for creat-
223 ing the Foldseek logo.

224 M.S. acknowledges support from the National Research
225 Foundation of Korea grants [2019R1A6A1A10073437,
226 2020M3A9G7103933, 2021R1C1C102065, 2021M3A9-
227 I4021220]; and the Creative-Pioneering Researchers Program
228 through Seoul National University. S.K. acknowledges
229 support by the National Research Foundation of Korea
230 (NRF) grant No. 2019R1A6A1A10073437. M.M. and J.S.
231 acknowledge support by the German ministry for education
232 and research (BMBF) via grant horizontal4meta.

233 This work used the Scientific Compute Cluster at GWDG,
234 the joint data center of Max Planck Society for the Advance-
235 ment of Science (MPG) and University of Göttingen.

236

Author contributions

237 M.K., S.K., J.S. & M.S. designed research. M.K., S.K.,
238 C.T., & M.S. developed code and performed analyses. M.K.
239 and J.S. developed the 3Di alphabet. M.M. developed the
240 webserver. M.K., S.K., C.T., M.M., J.S. & M.S. wrote the
241 manuscript.

242

Competing financial interests

243 The authors declare no competing financial interests.

244

METHODS

245 **Overview** Foldseek enables fast and sensitive comparison of
246 large structure sets. It encodes structures as sequences over
247 the 20-state 3Di alphabet and thereby reduces structural align-
248 ments to 3Di sequence alignments. The 3Di alphabet devel-
249 oped for Foldseek describes tertiary residue-residue interac-
250 tions instead of backbone conformations and proved critical
251 for reaching high sensitivities. Foldseek’s prefilter finds two
252 *similar*, spaced 3Di *k*-mer matches in the same diagonal of
253 the dynamic programming matrix. By not restricting itself to
254 exact matches, the prefilter achieves high sensitivity while re-
255 ducing the number of sequences for which full alignments are
256 computed by several orders of magnitude. Further speed-ups
257 are achieved by multi-threading and utilizing single instruction
258 multiple data (SIMD) vector units. Owing to the SIMDe li-
259 brary (github.com/simd-everywhere/simde), Foldseek runs on
260 a wide range of CPU architectures (x86_64, arm64, ppc64le)
261 and operating systems (Linux, macOS). The core modules of
262 Foldseek, which build on the MMseqs2 framework [22], are de-
263 scribed in the following paragraphs.

264 **Create database** The `createdb` module converts a set of
265 Protein Data Bank (PDB; [23]) or macromolecular Crystal-
266 lographic Information File (mmCIF) formatted files into an
267 internal Foldseek database format using the `gemmi` package
268 (project-gemmi.github.io). The format is compatible with
269 the MMseqs2 database format, which is optimized for paral-
270 lel access. We store each chain as a separate entry in the
271 database. The module follows the MMseqs2 `createdb` mod-
272 ule logic, however, in addition to the amino acid sequence it
273 computes the 3Di sequence from the 3D atom coordinates of
274 the C_α and C_β , C_{backbone} and N coordinates (see “Descrip-
275 tors for 3Di structural alphabet”). The 3Di and amino acid
276 sequence, and the C_α floating-point coordinates are stored in
277 the database.

278 **Prefilter** The `prefilter` module generates similar k-mers
279 and detects double, consecutive, similar k-mer matches that
280 occur on the same diagonal. In contrast to the MMseqs2
281 prefilter, the Foldseek prefilter utilizes the 3Di information
282 instead of the amino acid sequence information to generate
283 similar k-mers using a 3Di substitution matrix (see “3Di sub-
284 stitution score matrix”). This criterion suppresses hits to
285 non-homologous structures effectively, as they are less likely
286 to have consecutive k-mer matches on the same diagonal by
287 chance. To counteract the effect of regions with 3Di composi-
288 tions that differ from the database average, a compositional
289 bias correction is applied in a way analogous to MMseqs2 [24].
290 For each hit we perform an ungapped alignment over the di-
291 agonals with double, consecutive, similar k-mer matches and
292 sort those by the maximum ungapped diagonal score. Align-
293 ments with a score of at least 15 bits are passed onto the next
294 stage.

295 **Pairwise local structural alignments** After the prefilter
296 has removed the vast majority of non-homologous sequences,
297 pairwise alignments are performed on the remaining sequences
298 in the `structurealign` module. Sequences are aligned us-
299 ing a SIMD accelerated Smith-Waterman algorithm [25, 26].

300 We extended this implementation to support amino acid and
301 3Di scoring, compositional bias correction, and 256-bit-wide
302 vectorization. The score linearly combines amino acid and
303 3Di substitution scores with weights 1.4 and 2.1, respectively.
304 A compositional bias correction is applied to the amino acid
305 and 3Di scores. To further suppress high-scoring false positive
306 matches, for each match we align the reversed query sequence
307 against the target and subtract the reverse score from the for-
308 ward score.

309 **E-Values** To estimate E-values for each match, we trained
310 a neural network to predict the mean μ and scale param-
311 eter λ of the extreme value distribution for each query. We
312 built a module in Foldseek called `computemulambda`, which
313 takes a query and database structures as input and aligns the
314 query against a randomly shuffled version of the database se-
315 quences. For each query sequence the module produces N
316 random alignments and fits to their scores an extreme-value
317 (Gumbel) distribution. The maximum likelihood fitting is
318 done using the Gumbel fitting function taken from HMMER3
319 (`hmmcalibrate`) [27]. To train the network, we predicted μ
320 and λ for 100 000 sequences sampled from the AlphaFoldDB.
321 We trained the network to predict μ and λ from the mono-
322 residue composition of the query and its length. The network
323 has 22 input nodes, 2 fully-connected layers with 32 nodes
324 each (ReLU activation) and two linear output nodes. The op-
325 timizer ADAM with learning rate 0.001 was used for training.
326 When testing the resulting E-values on searches with scram-
327 bled sequences, the log of the mean number of false positives
328 per query turned out to have an accurately linear dependence
329 on the log of the reported E-values, albeit with a slope of 0.32
330 instead of 1. We therefore correct the E-values from the neural
331 network by taking them to the power of 0.32. We compared
332 how well the mean number of FPs at a given E-value agreed
333 with the E-values reported by Foldseek, MMseqs2, and 3D-
334 Blast, (**Fig. 2c** for SCOPe and **Supplementary Fig. 6** for
335 AlphaFoldDB). We considered a hit as FP if it was in a dif-
336 ferent fold and had a TM-score lower than 0.3. Furthermore,
337 we ignored all cross-fold hits within the four- to eight-bladed
338 β -propeller superfamilies (SCOPe b.66-b.70) and within the
339 Rossman-like folds (c.2-c.5, c.27, c.28, c.30, and c.31) because
340 of the extensive cross-fold homologies within these groups [28].

Pairwise global structural alignments using TM-align

342 We also offer the option to use TM-align for pairwise align-
343 ments. We implemented TM-align based on the C_α atom co-
344 ordinates and made adjustments to improve the (1) speed and
345 (2) memory usage. (1) TM-align performs multiple floating-
346 point based Needleman-Wunsch (NW) alignment steps, while
347 applying different scoring functions (e.g., score secondary
348 structure, Euclidean distance of superposed structures or frag-
349 ments, etc.) TM-align’s NW code did not take advantage of
350 SIMD instructions, therefore, we replaced it by parasail’s [29]
351 SIMD-based NW implementation and extended it to support
352 the different scoring functions. We also replaced the TM-score
353 computation using `fast_protein_cluster`’s SIMD based imple-
354 mentation [30]. Our NW implementation does not compute
355 exactly the same alignment since we apply affine gap costs
356 while TM-align does not. (2) TMalign requires $17 \text{ bytes} \times$
357 $\text{query length} \times \text{target length}$ of memory, we reduce the con-

stant overhead from 17 to 4 bytes. If Foldseek is used in TM-align mode (parameter `--alignment-type 1`), we replace the reported E-value column with TM-scores normalized by the query length. The results are ordered in descending order by TM-score.

Descriptors for 3Di structural alphabet The 3Di alphabet describes the tertiary contacts between residues and their nearest neighbors in 3D space. For each residue i the conformation of the local backbone around i together with the local backbone around its nearest neighbor j is approximated by 20 discrete states (see **Supplementary Fig. 3**). We chose the alphabet size $A = 20$ as a trade-off between encoding as much information as possible (large A) and limiting the number of similar 3Di k -mers that we need to generate in the k -mer based prefilter. This number scales with A^k , giving us an alphabet size similar to the size of the amino acid alphabet. The discrete single-letter states are formed from neighborhood descriptors containing ten features encoding the conformation of backbones around residues i and j represented by the C_α atoms ($C_{\alpha,i-1}, C_{\alpha,i}, C_{\alpha,i+1}$) and ($C_{\alpha,j-1}, C_{\alpha,j}, C_{\alpha,j+1}$). The descriptors use the five unit vectors along the following directions,

$$\begin{aligned} u_1 : C_{\alpha,i-1} &\rightarrow C_{\alpha,i} & u_4 : C_{\alpha,j} &\rightarrow C_{\alpha,j+1} \\ u_2 : C_{\alpha,i} &\rightarrow C_{\alpha,i+1} & u_5 : C_{\alpha,i} &\rightarrow C_{\alpha,j} \\ u_3 : C_{\alpha,j-1} &\rightarrow C_{\alpha,j}. \end{aligned}$$

We define the angle between u_k and u_l as ϕ_{kl} , so $\cos \phi_{kl} = u_k^T u_l$. The seven features $\cos \phi_{12}$, $\cos \phi_{34}$, $\cos \phi_{15}$, $\cos \phi_{35}$, $\cos \phi_{14}$, $\cos \phi_{23}$, $\cos \phi_{13}$, and the distance $|C_{\alpha,i} - C_{\alpha,j}|$ describe the conformation between the backbone fragments. In addition, we encode the sequence distance with the two features $\text{sign}(i-j) \min(|i-j|, 4)$ and $\text{sign}(i-j) \log(|i-j| + 1)$.

Learning the 3Di states using a VQ-VAE The ten-dimensional descriptors were discretized into an alphabet of 20 states using a variational autoencoder with vector-quantized latent variables (VQ-VAE) [31]. In contrast to the standard VQ-VAE, we trained the VQ-VAE not as a simple generative model but rather to learn states that are maximally conserved in evolution. To that end, we trained it with pairs of descriptors $\mathbf{x}_n, \mathbf{y}_n \in \mathbb{R}^{10}$ from structurally aligned residues, to predict the distribution of \mathbf{y}_n from \mathbf{x}_n . The VQ-VAE consists of an encoder and decoder network with the discrete latent 3Di state as a bottleneck in-between. The encoder network embeds the 10-dimensional descriptor \mathbf{x}_n into a two-dimensional continuous latent space, where the embedding is then discretized by the nearest centroid, each centroid representing a 3Di state. Given the centroid, the decoder predicts the probability distribution of the descriptor \mathbf{y}_n of the aligned residue. After training, only encoder and centroids are used to discretize descriptors. Encoder and decoder networks are both fully connected with two hidden layers of dimension 10, a batch normalization after each hidden layer and ReLU as activation functions. The encoder, centroids, and decoder have 242, 40, and 352 parameters, respectively. The output layer of the decoder consists of 20 units predicting μ and σ^2 of the descriptors x of the aligned residue, such that the decoder predicts $\mathcal{N}(x|\mu, I\sigma^2)$ (with

diagonal covariance). We trained the VQ-VAE on the loss function defined in Equation (3) in [31] (with commitment loss = 0.25) using the deep-learning framework PyTorch (version 1.9.0), the ADAM optimizer, with a batch size of 512, and a learning rate of 10^{-3} over 4 epochs. Using Kerasify, we integrated the encoder network into Foldseek. The domains from the SCOPe database were split 80%/20% by fold into training and validation sets. For the training, we structurally aligned the structures with TMalign, removed all alignments with a TM-score below 0.6, and removed all aligned residue pairs with a distance between their C_α atoms of more than 5 Å. We trained the VQ-VAE with 100 different initial parameters and chose the model that was performing best in the benchmark on the validation dataset (the highest sum of ratios between 3Di AUC and TMalign AUC for family, superfamily and fold level).

3Di substitution score matrix We trained a BLOSUM-like substitution matrix for 3Di sequences from pairs of structurally aligned residues used for the “VAE-VQ training”. First, we determined the 3Di states of all residues. Next, the substitution frequencies between 3Di states were calculated by counting how often two 3Di states were structurally aligned. (Note that the substitution frequencies from state A to B and the opposite direction are equal.) Finally, the score $S(x, y) = 2 \log_2 \frac{p(x, y)}{p(x)p(y)}$ for substituting state x through state y is the log-ratio between the substitution frequency $p(x, y)$ and the probability that the two states occur independently, scaled by the factor 2.

Optimize nearest-neighbor selection To select nearest-neighbor residues that maximize the performance of the resulting 3Di alphabet in finding and aligning homologous structures, we introduced the virtual center V of a residue. The virtual center position is defined by the angle θ ($V-C_\alpha-C_\beta$), the dihedral angle τ ($V-C_\alpha-C_\beta-N$), and the length l ($|V-C_\alpha|$). For each residue i we selected the residue j with the smallest distance between their virtual centers. The virtual center was optimized on the training and validation structure sets used for the VQ-VAE training by creating alphabets for positions with $\theta \in [0, 2\pi]$, $\tau \in [-\pi, \pi]$ in 45° steps, and $l \in \{1.53\text{Å} k : k \in \{1, 1.5, 2, 2.5, 3\}\}$ (1.53Å is the distance between C_α and C_β). The virtual center defined by $\theta = 270^\circ$, $\tau = 0^\circ$ and $l = 2$ performed best in the benchmark. For glycines, the C_β positions were approximated by forming a tetrahedral from C_α . This virtual center preferably selects long-range, tertiary interactions and only falls back to selecting interactions to $i+1$ or $i-1$ when no other residues are nearby. In that case, the interaction captures only the backbone conformation.

SCOPe Benchmark We downloaded SCOPe 2.07 [32] structures, clustered at 40% sequence identity, containing 11 211 domains, for the generation of 3Di states and for the performance evaluation of Foldseek. The SCOPe benchmark set consists of single domains with an average length of 174 residues. In our benchmark, we compare the domains all-versus-all. Per domain, we measured the fraction of detected TPs up to the 5th false positive. For family-, superfamily- and fold-level recognition, TPs were defined as same family, same superfamily and not same family, and same fold and

not same superfamily, respectively. Hits from different folds are FPs.

AlphaFold database used for all-versus-all search We downloaded the AlphaFoldDB [33] version 1 containing 365,198 protein models and searched it all-versus-all using Foldseek -s 9.5 --max-seqs 2000. For our second best hit analysis we consider only models with: (1) an average C_α 's pLDDT greater than or equal to 80, and (2) models of non-fragmented domains. We also computed the structural similarity for each pair using TMalign (default options).

Performance evaluation: Sensitivity In order to evaluate the sensitivity of the structural alignment tools, we used a cumulative ROC curve analysis. After sorting the alignment result of each query, we calculated the fraction of TPs in the list up to the 5th false positives. We qualitatively measured the sensitivity by comparing the area under the curve (AUC) for family-, superfamily-, and fold-level classifications.

Performance evaluation: Runtime Using the SCOPe benchmark dataset, the runtime of the pairwise structural alignment was evaluated for all methods. Depending on the processing time of each tool, the runtimes of the structural alignment tools TM-align, DALI, and CE were estimated on 10% of the benchmark set (1121 proteins randomly selected from the SCOPe domains). Tools with multi-threading support (MMseqs2 and Foldseek) were executed with 64 threads, tools without were parallelized by breaking the query set into 64 equally sized chunks and executing them in parallel.

Tools and options for benchmark comparison Following are command lines used in the SCOPe benchmark.

Foldseek We used Foldseek commit 4de45 during this analysis. Foldseek was run with the following parameters: --threads 64 -s 9.5 -e 10 --max-seqs 2000

MMseqs2 We used the default MMseqs2 (release 13-45111) search algorithm to obtain the sequence-based alignment result. MMseqs2 sorts the results by e-value and score. We searched with: --threads 64 -s 7.5 -e 10000 --max-seqs 2000

CLE-Smith-Waterman We used PDB Tool v4.80 (github.com/realbigws/PDB_Tool) to convert the benchmark structure set to CLE sequences. After the conversion, we used SSW [26] (commit ad452e) to align CLE sequences all-versus-all. We sorted the results by alignment score. The following parameters were used to run SSW: (1) protein alignment mode (-p), (2) gap open penalty of 100 (-o 100), (3) gap extend penalty of 10 (-e 10), (4) CLE's optimized substitution matrix (-a cle.shen.mat), (5) returning alignment (-c). The gap open and extend values were inferred from DeepAlign [34]. The results are sorted by score in descending order.

```
ssw_test -p -o 100 -e 10 -a cle.shen.mat -c
```

3D-BLAST We used 3D-BLAST (beta102) with BLAST+ (2.2.26) and SSW [26] (version ad452e). We first converted the PDB structures to a 3D-BLAST database using 3d-blast -sq_write and 3d-blast -sq_append. We searched the structural sequences against the database using blastp with the following parameters: (1) we used 3D-BLAST's

optimized substitution matrix (-M 3DBLAST), (2) number of hits and alignments shown of 12000 (-v 12000 -b 12000), (3) E-value threshold of 1000 (-e 1000) (4) disabling query sequence filter (-F F) (5) gap open of 8 (-G 8), and (6) gap extend of 2 (-E 2). 3D-BLAST's results are sorted by E-value in ascending order:

```
blastall -p blastp -M 3DBLAST -v 12000 -b 12000 -e 1000 -F F -G 8 -E 2
```

For Smith-Waterman we used (1) gap open of 8 (2) gap extend of 2 and (3) returning alignments (-c) (4) using the 3D-BLAST's optimized substitution matrix (-a 3DBLAST), (5) protein alignment mode (-p): ssw_test -o 8 -e 2 -c -a 3DBLAST -p. Presented in Figure 2 are the Smith-Waterman results, since BLAST performed worse with an average AUC of 0.573, 0.127, 0.009 for family-, superfamily- and fold-classification, respectively.

TMalign We downloaded and compiled the TMalign.cpp source code (version 2019/08/22) from the Zhang group website. We ran the benchmark using default parameters and -fast for the fast version. We used the TM score normalized by the 1st chain (query) in all our analyses. Default: TMalign query.pdb target.pdb
Fast: TMalign query.pdb target.pdb -fast

DALI We installed the standalone DaliLite.v5. For the SCOPe benchmark set, input files were formatted in DAT files with DALI's import.pl. The conversion to DAT format produced 11137 valid structures out of the 11211 initial structures for the SCOPe benchmark. After formatting the input files, we calculated the protein alignment with DALI's structural alignment algorithm. The results were sorted by DALI's Z-score:

```
import.pl -pdbfile query.pdb -pdbname PDBid -dat DAT dali.pl -cd1 queryDATid -db targetDB.list -TITLE systematic -dat1 DAT -dat2 DAT -outfmt "summary" -clean
```

CE We used BioJava's [35] (version 5.4.0) implementation of the combinatorial extension (CE) alignment algorithm. We modified one of the modules of BioJava under shape configuration to calculate the CE value. Our modified CEalign.jar file requires a list of query files, path to the target PDB files, and an output path as input parameters. This Java module runs an all-versus-all CE calculation. The Jar file of our implementation of CE calculation is provided.
java -jar CEalign.jar querylist.txt TargetPDBDirectory OutputDirectory

Hardware specifications for benchmarks The runtime benchmarks were executed on a machine with an AMD EPYC 7702P 64-core CPU and 1024 GB RAM memory.

Webserver The Foldseek webserver is a continuation of the MMseqs2 webserver [36]. To allow for searches in seconds we implemented MMseqs2's pre-computed database indexing capabilities in Foldseek. Using these, the search databases can be held fully in system memory by the operating system and instantly accessed by each Foldseek process, thus avoiding expensive accesses to slow disk drives. A similar mechanism was used to store and read the associated taxonomic information. The AlphaFoldDB/Proteome (v1), AlphaFoldDB/Swiss-Prot

582 (v2), and PDB100 require 3.9GB, 3.6GB, and 2.2GB RAM,
583 respectively. The databases are kept in memory using
584 vmtouch (github.com/hoytech/vmtouch).

585 **Code availability** Foldseek is GPLv3-licensed free open
586 source software. The source code and binaries for Foldseek can
587 be downloaded at github.com/steineggerlab/foldseek.
588 The webserver code is available at github.com/soedinglab/mmseqs2-app. The analysis scripts are available at:
589 github.com/steineggerlab/foldseek-analysis.

590 **Data availability** Benchmark data and Foldseek databases
591 are available at: wwwuser.gwdg.de/~compbiol/foldseek.

593

REFERENCES

- 594 [22] Steinegger, M. & Söding, J. *Nat Biotechnol* **35**, 1026–1028
595 (2017).
- 596 [23] Burley, S. K. *et al. Nucleic Acids Res* **47**, D520–D528 (2019).
- 597 [24] Hauser, M. *et al. Bioinformatics* **32**, 1323–1330 (2016).
- 598 [25] Farrar, M. *Bioinformatics* **23**, 156–161 (2007).
- 599 [26] Zhao, M. *et al. PLOS One* **8**, e82138 (2013).
- 600 [27] Eddy, S. R. *PLOS Comput Biol* **7**, e1002195 (2011).
- 601 [28] Söding, J. & Remmert, M. *Curr Opin Struct Biol* **21**, 404–411
602 (2011).
- 603 [29] Daily, J. *BMC Bioinform* **17**, 81 (2016).
- 604 [30] Hung, L.-H. & Samudrala, R. *Bioinformatics* **30**, 1774–1776
605 (2014).
- 606 [31] Van den Oord, A. *et al. Adv Neur Inf Proc Syst (NIPS)* **30**
607 (2017).
- 608 [32] Chandonia, J.-M. *et al. Nucleic Acids Res* **47**, D475–D481
609 (2019).
- 610 [33] Varadi, M. *et al. Nucleic Acids Res* **50**, D439–D444 (2022).
- 611 [34] Jiménez-Moreno, A. *et al. J Struct Biol* **213**, 107712 (2021).
- 612 [35] Lafita, A. *et al. PLOS Comput Biol* **15**, e1006791 (2019).
- 613 [36] Mirdita, M. *et al. Bioinformatics* **35**, 2856–2858 (2019).